Science of the Total Environment 668 (2019) 216–223

Contents lists available at ScienceDirect

Science of the Total Environment

journal homepage: www.elsevier.com/locate/scitotenv

Biogeochemical fate of ferrihydrite-model organic compound complexes during anaerobic microbial reduction

Dawit N. Wordofa [a], Dinesh Adhikari [a,1], Sarrah M. Dunham-Cheatham [a,b], Qian Zhao [a,c], Simon R. Poulson [d], Yuanzhi Tang [e], Yu Yang [a,*]

[a] Department of Civil and Environmental Engineering, University of Nevada, Reno, NV 89557, USA
[b] Department of Natural Resources and Environmental Science, University of Nevada, Reno, NV 89557, USA
[c] Pacific Northwest National Laboratory, Richland, WA 99354, USA
[d] Department of Geological Sciences and Engineering, University of Nevada, Reno, NV 89557, USA
[e] School of Earth and Atmospheric Sciences, Georgia Institute of Technology, Atlanta, GA 30332, USA

HIGHLIGHTS

- Benzoquinone facilitated reduction of ferrihydrite most greatly.
- Benzoquinone acted as an electron shuttle.
- Organic carbon can also affect the microbial activities for iron reduction.

GRAPHICAL ABSTRACT

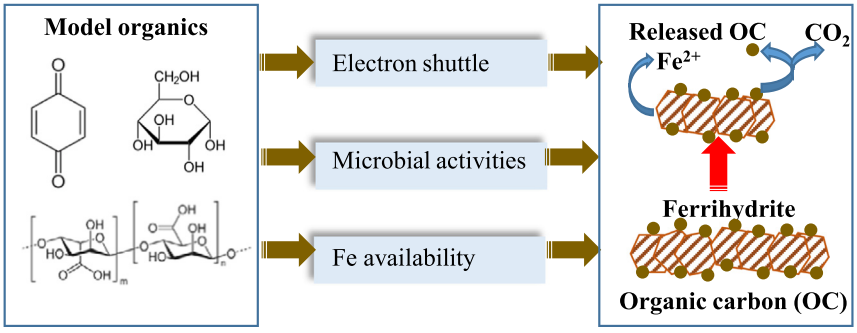

ARTICLE INFO

Article history:
Received 21 January 2019
Received in revised form 25 February 2019
Accepted 27 February 2019
Available online 01 March 2019

Editor: Jay Gan

Keywords:
Ferrihydrite
Microbial reduction
Organic carbon
Quinone
Electron transport

ABSTRACT

Associations of organic carbon (OC) with iron (Fe) oxide minerals play an important role in regulating the stability of OC in soil environments. Knowledge about the fate and stability of Fe-OC complexes is impaired by the heterogeneity of OC. Additional biogeochemical variables in soil environments, such as redox conditions and microbes, further increase complexity in understanding the stability of mineral-associated soil OC. This study investigated the fate and stability of model organic compounds, including glucose (GL), glucosamine (GN), tyrosine (TN), benzoquinone (BQ), amylose (AM), and alginate (AL), complexed with an Fe oxide mineral, ferrihydrite (Fh), during microbial reduction. During a 25-d anaerobic incubation with *Shewanella putrefaciens* CN32, the reduction of Fe followed the order of Fh-BQ > Fh-GL > Fh-GN > Fh-TN > Fh-AL > Fh-AM. In terms of OC released during the anaerobic incubation, Fh-GN complexes released the highest amount of OC while Fh-AM complexes released the lowest. Organic carbon regulated the reduction of Fe by acting as an electron shuttle, affecting microbial activities, and associating with Fh. Benzoquinone had the highest electron accepting capacity, but potentially can inhibit microbial activity. These findings provide insights into the roles of different organic functional groups in regulating Fe reduction and the stability of Fh-bound OC under anaerobic conditions.

* Corresponding author.
E-mail address: yuy@unr.edu (Y. Yang).
[1] Current address: Lawrence Livermore National Laboratory, 7000 East Ave, Livermore, CA 94550, USA.

https://doi.org/10.1016/j.scitotenv.2019.02.441
0048-9697/

1. Introduction

Soil represents one of the prevalent carbon (C) reservoirs on Earth and plays an enormous role in the global C cycle and climate change (Scurlock and Hall, 2008). As soil organic carbon (OC) represents a substantial fraction of C in terrestrial ecosystems, long-term storage of soil OC is crucial for the mitigation of carbon dioxide (CO_2) emissions from anthropogenic and natural sources (Gál et al., 2007; Meersmans et al., 2009). Hence, understanding the stability of soil OC is imperative to understand and quantitatively predict the C cycle and its response to climate change.

Previous studies have demonstrated that associations between iron (Fe) oxides and OC are important for regulating the fate and stability of OC in soils (Adhikari et al., 2019a, 2019b, 2017, 2016; Adhikari and Yang, 2015; Hall et al., 2016; Pan et al., 2016; Porras et al., 2018; Zhao et al., 2016, 2017). Iron-bound OC represents a substantial fraction of total soil OC (Kaiser and Guggenberger, 2000; Lalonde et al., 2012; Wagai and Mayer, 2007; Zhao et al., 2017). Under reducing conditions, Fe-bound OC can be reductively released to the solution phase and undergo potential subsequent reactions (Adhikari et al., 2016; Adhikari and Yang, 2015; Grybos et al., 2007; Huang and Hall, 2017). During the oxidation of Fe(II) to Fe(III), OC in the solution phase can be oxidized to CO_2 or re-incorporated into Fe-OC complexes (Chen and Thompson, 2018; Ginn et al., 2017; Huang et al., 2018; Pan et al., 2016). However, knowledge about the associations between Fe minerals and OC and their impact on soil OC dynamics is far from complete, partially because the chemical composition of soil OC is highly heterogeneous and lacks clearly-defined molecular structures.

The functional groups present in OC can interact with Fe oxides and impact how Fe oxides behave under reducing conditions (Han et al., 2016; Liptzin and Silver, 2009). Quinone moieties have been identified as a critical functional group mediating extracellular electron transport for Fe reduction (Li et al., 2013; O'Loughlin, 2008; Roden et al., 2010; Taran, 2017). Carboxylic functional groups can bind with Fe oxides through both inner- and outer-sphere coordination complexation, which potentially can influence microbial bioavailability and reduction kinetics of Fe oxides (Cornell, 1985; Dippold et al., 2014). Other hydrophilic functional groups, such as hydroxyl groups in carbohydrates, can potentially influence Fe reduction through weaker interactions, such as van der Waals interactions and hydrogen bonding (Adhikari et al., 2019a, 2019b). In addition, the molecular size of organic compounds can influence their interactions with Fe oxides (Chorover and Amistadi, 2001; Philippe and Schaumann, 2014). Achieving a more accurate process-based understanding of the fate of Fe-bound OC requires further investigation of the dynamics of specific Fe-bound functional groups during microbial reduction.

In this study, we systematically investigated the fate of ferrihydrite (Fh)-bound organic compounds containing different functional groups under reducing conditions in the presence of an Fe-reducing bacterium, *Shewanella putrefaciens* CN32 (CN32). Ferrihydrite was used as a representative Fe oxide, as it is ubiquitous in soils especially Spodosols and OC-enriched soils (Cornell and Schwertmann, 1996; Jambor and Dutrizac, 1998). Ferrihydrite was co-precipitated with representative model organic compounds to form mineral-OC complexes, and are hereafter referred to as ferrihydrite-benzoquinone (Fh-BQ), ferrihydrite-glucose (Fh-GL), ferrihydrite-glucosamine (Fh-GN), ferrihydrite-tyrosine (Fh-TN), ferrihydrite-amylose (Fh-AM), and ferrihdrite-alginate (Fh-AL) (Supporting Information (SI), Table S1). These organic compounds were selected as they represent a range of functional groups and moieties existing in the natural environment, including quinones, hydroxyls, carboxylic acids, and amine/carboxylic acid in amino acids. The use of Fh-AM and Fh-AL complexes can shed light on the role of large molecules in Fe oxide behavior under microbial reducing conditions, whereas Fh-BQ, Fh-GL, Fh-GN, and Fh-TN complexes can provide information on the role of low-molecular-weight compounds (< 1000 Da). The kinetics for microbial Fe reduction and changes in Fe speciation have been analyzed, and the release and transformation of OC have also been studied.

2. Materials and method

2.1. Materials

The chemicals used in this study were reagent grade and purchased from either Sigma Aldrich or Fisher Scientific, unless stated otherwise. Ferric chloride hexahydrate ($FeCl_3{\cdot}6H_2O$) (Amresco) was used to prepare Fh and Fh-organic compound complexes. α-D(+)-glucose anhydrous (Acros Chemicals>99%), p-benzoquinone (Alfa Aesar, >98%), glucosamine hydrochloride (>99%), sodium alginic salt (>99.5%), amylose from potato (ACS grade), and L-tyrosine (>99%) were used to synthesize Fh-organic compound complexes. Piperazine-*N*,*N*′-bis(2-ethanesulfonic acid) (PIPES) buffer (bioWORLD) and ferrozine were used to prepare the Fe assay reagent, following our studies (Adhikari et al., 2016, 2017).

2.2. Fh-organic compound complex synthesis

Fh-organic compound complexes were synthesized by co-precipitating Fh with one of the organic compounds at a feed C/Fe molar ratio of 1:1, following our previous studies (Adhikari et al., 2017, 2019a, 2019b). To synthesize 2-line Fh and Fh-organic compound complexes, 5.4 g $FeCl_3{\cdot}6H_2O$ was dissolved in 200 mL double deionized (DDI) water (18 MΩ·cm) in the absence and presence of model organic compounds with pre-determined concentrations. The pH of the solution was adjusted to 7.5 by adding 0.5 M NaOH, while being magnetically stirred (Adhikari et al., 2017). Once the pH was stable at 7.5, the precipitated particles were allowed to settle for 20 min, and the supernatant was decanted. The precipitated particles were mixed with 600 mL DDI, the solution was magnetically stirred, and supernatant was decanted after gravitational settling of the particles. The rinse with DDI was repeated 5 more times to remove salts. Washed samples were centrifuged at 10,000 rcf for 10 min, and the supernatant was decanted. The wet precipitates were kept at 4 °C for further experiments. The C/Fe molar ratio of the resulting complexes was examined by analysis of OC and Fe content upon complete dissolution of the complexes with 2 M HCl (SI, Fig. S1). The OC concentration was determined by dissolved OC (DOC) analysis with a Shimadzu TOC-VCSH (Kyoto, KYT, Japan). The Fe concentration was determined by reducing the dissolved Fe with hydroxylamine hydrochloride (10% *w*/*v* hydroxylamine hydrochloride in 1 M HCl) and measuring the subsequent Fe(II) concentration using the ferrozine assay (1% w/v ferrozine in 50% w/v ammonium acetate) (Adhikari et al., 2017; Stookey, 1970; Xu et al., 2016).

2.3. Microbial Fe reduction

Shewanella putrefaciens CN32 (CN32), a model dissimilatory metal reducing bacterium extensively investigated, was used in this study for the microbial reduction of Fe to mimic naturally occurring redox reactions (Fredrickson et al., 1998; Najem et al., 2016; Roden, 2003, 2004; Zhao et al., 2017). Pure cultures were maintained under aerobic conditions on Luria Broth (LB) agar at 4 °C. Cells were transferred to sterile LB medium (25 g L^{-1}) and incubated at 30 °C for 14–16 h to achieve stationary phase. Cells were centrifuged at 10,000 rcf for 5 min, and the remaining medium was decanted. The cell pellets were then washed three times with 3 M sodium bicarbonate buffer ($NaHCO_3$, pH 7.0 ± 0.1) by adding 40 mL of freshly prepared buffer to the pellet, vortexing the mixture to achieve homogeneity, and then centrifuging the suspension at 10,000 rcf for 5 min for each wash. The washed cells were re-suspended in bicarbonate buffer (3 M, pH 7.0) to achieve a cell slurry with an optical density (OD600) of 0.9, equivalent to a cell density of $10^{8.5}$ cells mL^{-1} (determined by replicate cell counts). Ferrihydrite-model compound complexes were added to the cell slurry at a concentration of around 575 mg C L^{-1} slurry, and the 10 mL of the resulting

suspension was crimp-sealed in a 20 mL serum bottle using an air-tight butyl rubber stopper under N_2/H_2 (96:4, *v*/v) headspace. Biotic controls were made using the same method, but utilizing non-complexed Fh (2300 mg Fe L^{-1}) instead of a Fh-model compound complex, to determine how the presence of OC affects the behavior of Fh. Bacteria controls were used to assess the contribution of Fe and OC from the bacterial cells alone, and were made using the cell slurry without any additional Fh or model organic compounds following the method above. The H_2 in the headspace of all suspensions and controls was introduced as an electron donor to facilitate the microbial reduction of Fe (Luan et al., 2010; Meshulam-Simon et al., 2007; Roden, 2004, 2003). Vials were incubated in a dark room on a 100 rpm shaking table for 25 days. Triplicates of all suspensions and controls were used in the incubation experiments.

2.4. Iron reduction kinetic analysis

At different intervals within the 25-day incubation (2, 4, 8, 10, 16, 20, and 25 days), samples were harvested for analysis of Fe reduction kinetics. Ferrous iron (Fe(II)) was quantified using the ferrozine assay. The ferrozine reagent was prepared by mixing 1 g of ferrozine with 50 mL of 1 M PIPES buffer and brought to a final volume of 1 L with DDI (Lovley and Phillips, 1986). The pH of the reagent was adjusted to 7.0 ± 0.1 by titration with 0.5 M NaOH. Harvested samples were centrifuged at 21,000 rcf for 5 min inside a glove box (96% N_2 and 4% H_2). To quantify the aqueous-phase Fe(II) concentration in the supernatants, 40 μL of supernatant was added to 4 mL of ferrozine reagent and 360 μL of DDI. The sample was vortexed. After 10-min static reaction, absorbance was measured by a UV–Vis spectrophotometer (Evolution 260 BIO, Thermo Scientific) at a wavelength of 562 nm. Calibration curves were generated using ferrous chloride. Sorbed Fe(II) was measured by adding HCl to a 5 mL aliquot of Fh-model organic compound complex slurry to achieve a concentration of 0.5 M HCl. The acidified complex slurry was agitated on a rotary shaker at 100 rpm for 12 h to dissolve all sorbed Fe(II). The concentration of Fe(II) in the acidified supernatant was measured using the same ferrozine assay method as described above. The sorbed-phase Fe(II) concentration was calculated as the difference between the Fe(II) concentration in the acidified supernatant minus the aqueous-phase Fe (II) concentration.

2.5. X-ray absorption spectroscopy

The speciation of Fe in each Fh-organic compound complex was studied by Fe K-edge X-ray absorption near edge structure (XANES) at Beamline 12-BM-B at Advanced Photon Source (APS), Argonne National Laboratory, Lemont, IL. Fine powders of samples were mounted in a sample holder sealed by Kapton tape and placed into a helium-purged chamber to maintain anaerobic conditions and prevent changes in Fe oxidation state. The beamline was equipped with a Lytle detector, and energy was calibrated against Fe foil at 7112 eV. Data analysis was performed using the software SixPack and Ifeffit (Newville, 2001; Webb, 2005).

2.6. X-ray diffraction (XRD)

The mineralogy of Fh and Fh-model compound complexes were confirmed using a powered X-ray diffractometer (XRD) (Bruker AXS, Karlsruhe, Germany). Synthesized Fh-model compound complexes were dried and ground to make a fine, homogenous powder. A small aliquot of the powder (50–100 mg) was loaded on a clean, zero-background glass slide and placed on the XRD sample holder for analysis. All samples were analyzed for the 2θ range of 20-90° with a step size of 0.02°.

2.7. Organic carbon release and transformation analysis

The transformation and release of OC into the solution phase in conjunction with microbial reduction of Fh-model compound complexes were analyzed at different intervals during the 25-day incubation. First, the concentration of gaseous carbon dioxide (CO_2) in the vial headspaces was analyzed using an infrared gas analyzer (IRGA; LI-8100A). Replicate ($n = 3$) vial headspace samples (100 μL) were collected using an air-tight micro-needle syringe and manually injected into the IRGA. A calibration curve was established by injecting CO_2 standards of varying concentrations. CO_2 standards were purchased from Norlab Specialty Gases (Norco, Inc., Boise, ID, USA). Then the suspension was centrifuged at 14,000 rcf for 10 min and the DOC in supernatants was quantified by Shimadzu TOC-VCSH analyzer (Kyoto, KYT, Japan). Following our previous studies (Adhikari et al., 2017, 2019a), the release of OC in samples with complexes was calibrated based on the biotic control, for which only Fh was mixed with the same concentration of CN32 as in the samples. In addition, methane (CH_4) concentrations in the headspace were measured using a European Greenhouse Gas Chromatograph (GC) System (SRI Instruments, Germany) equipped with a flame ionization detector. The instrument was calibrated using CH_4 standards in the range of 0.1–50,000 mg L^{-1}. For CH_4 analysis, headspace air was directly sampled through a hypodermic needle attached to the sample coil.

2.8. Electron accepting capacity (EAC)

The electron accepting capacity (EAC) of the organic compounds in the Fh-organic compound complexes was quantified to estimate the capacity of the compound to act as an electron shuttle between bacteria and Fh in the suspensions. Electron shuttling processes, i.e. that microbially reduced OC can consequently donate electrons to metals, have been extensively demonstrated important for redox reactions of Fe (Kappler et al., 2004; Bose et al., 2009; Roden et al., 2010). EACs of each organic compound and Fh-organic compound complex were measured to quantify the EAC of free OC and Fh-bound OC, respectively. Ferric nitrilotriacetic acid (Fe(III)-NTA) solution was prepared by mixing 1.69 g of $NaHCO_3$, 2.57 g of trisodium nitrilotriacetic acid (Na_3NTA) and 2.79 g of $FeCl_3$ in 100 mL of DDI water. The solution of OC or Fh-bound OC was mixed with CN32 (final suspension OD600 = 0.8) and sealed in air-tight bottles under headspace of 96% N_2 and 4% H_2, as the electron donor for the Fe reduction (Adhikari et al., 2017; Chacon et al., 2006). The suspensions were shaken on a table shaker at 100 rpm in a dark room. At different intervals, 0.25 mL of the suspension was filtered through a 0.45 μm glass fiber filter and reacted with 2 mL of 5 mM Fe(III)-NTA for 1 min (Adhikari et al., 2017; Lovly et al., 1996; Roden et al., 2010). After 1 min, the mixture was filtered through a 0.25 μm glass fiber filter and 0.5 mL of the filtrate was mixed with 5 mL of 1 g L^{-1} ferrozine solution to quantify the Fe(II) concentration (see ferrozine method above, Section 2.2). The Fe(II) concentration of the filtrate corresponds to the EAC of OC in either the free, non-mineral-bound model compounds or Fh-bound model compound complexes.

2.9. Impact of organic compounds on bacterial growth

The impact of each model organic compound on the growth of CN32 was studied as an indicator of the potential influences on microbial activities. Cells were sterilely transferred to LB medium containing model organic compounds (960 mg C L^{-1}) and incubated at 30 °C for up to 96 h. At different time intervals, the cell density (OD600) of the cell suspension was quantified. In addition, pre-incubated cells at stationary phase in LB medium were mixed with sterile DDI to achieve an optical density of 1.0 and model organic compounds were added (960 mg C L^{-1} added from the compound). The suspensions were incubated at 30 °C for up to 75 h, and the optical density was measured regularly throughout the incubation.

In the presence of OC, the growth kinetics of CN32 were fitted using a modified logistic model, incorporating population decay (Eq. (1)) ($R^2 = 0.89–0.95$):

$$y = \frac{A}{\left\{1 + \exp\left[\frac{4\mu_m}{A}(\lambda - t) + 2\right]\right\}} \exp(-dt) \quad (1)$$

where y is the OD_{600} for relative microbial population size, μ_m is the maximum specific growth rate (hr^{-1}), λis the lag time (hr), A is the maximal population size, d is the death rate after the lag phase (hr^{-1}), and t is the incubation time (hr).

2.10. Statistical analysis

Statistical analysis (t-test and Pearson correlation analysis) were performed with IBM SPSS Statistics 24. Empirical model fittings were done with Matlab 2013, and linear regression was conducted with Microsoft Excel 2016.

3. Results

3.1. Iron reduction

Within the 25-day incubation, a substantial amount of Fe (14.5 ± 0.26 to 54.7 ± 1.05% of the total Fe added) was reduced, with 32.1–46.3% of measured Fe(II) released to the solution phase and the remaining measured Fe(II) sorbed by residual complexes and/or bacteria (Fig. 1). The fraction of total measured Fe(II) to total Fe followed the order of Fh-BQ (54.7%) > Fh-GL (29.3%) > Fh-GN (23.6%) > Fh-TN (19.6%) > Fh-AL (18.5%) > Fh-AM (15.0%) > Fh (14.5%) (Fig. 1). For Fh-BQ, 435 ± 2 mg dissolved Fe(II) L^{-1} and 1451 ± 38 mg sorbed Fe(II) L^{-1} were produced during the 25-day incubation, compared to 42 ± 4 mg dissolved Fe(II) L^{-1} and 295 ± 12 mg sorbed Fe(II) L^{-1} for the biotic control, which contained pure Fh. The abiotic control (Fh-model organic compound complexes without the addition of CN32) showed minimal reduction (<5% total Fe reduced) (SI, Fig. S2). Based on linear regression analysis of Fe reduction versus time, the total Fe reduction rate ranged between 12 and 80 mg L^{-1} d^{-1} (SI, Table S2).

3.2. Iron speciation

The Fe mineral phase in all original Fh-model organic compound complexes was confirmed to be Fh by XRD (SI, Fig. S3). For Fh-TN, there were additional peaks in the XRD spectrum attributed to TN (SI, Fig. S3, Fh-TN), suggesting TN was either precipitated or crystallized together with the Fh. XANES results indicate a change in the oxidation state of Fe during the anaerobic microbial incubation for some complexes (Fig. 2). For instance, the XANES white line peak position clearly shifted from 7132 A^{-1} to 7130 A^{-1} for Fh-AL after reduction (Fig. 2E).

3.3. Release of Fe-bound OC

In conjunction with Fe reduction, up to 45.2 ± 0.2% of Fh-bound OC was released to the solution phase within 25 days (Fig. 3). The release of Fh-bound OC followed the order Fh-BQ > Fh-GN > Fh-TN > Fh-GL > Fh-AL ≈ Fh-AM. The preferential release index (PRI), defined as the ratio of (dissolved OC (DOC)/total OC (TOC))/(total Fe(II)/total Fe), ranged from 0.7 to 1.6 (SI, Fig. S4). This index is used as an indication of preferential release of OC relative to the reduction of Fe, with a higher value representing favored release of OC compared to the reduction of Fe. Fh-GN and Fh-TN had PRI values above 1, indicating the release fraction of OC was higher than that for the reduction of Fe, whereas Fh-BQ, Fh-GL, Fh-Al, and Fh-AM had PRI values below 1, indicating the Fe reduction fraction over the release of OC.

The concentration of DOC was strongly correlated with the concentration of total Fe(II) (Pearson correlation coefficient $r = 0.92–0.98$, $p < 0.01$) and dissolved Fe(II) ($r = 0.84–0.96$, $p < 0.01$) (Fig. 4, SI, Table S3). The correlation was also strong between the fraction of DOC in TOC and the fraction of total Fe(II) in total Fe ($r = 0.92–0.99$, $p < 0.01$).

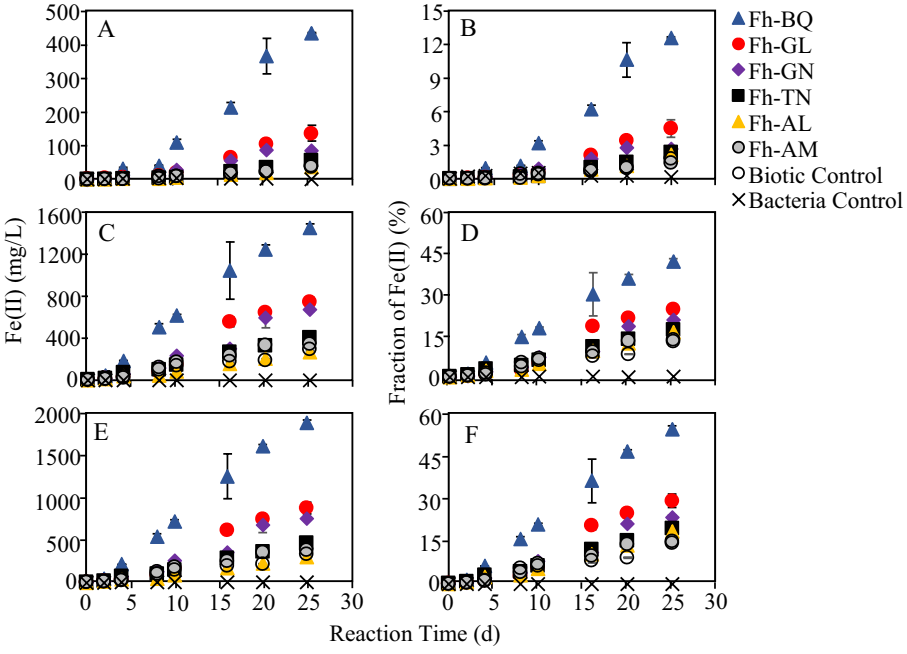

Fig. 1. Time-dependent generation of Fe(II) during the anaerobic incubation of ferrihydrite (Fh)-organic compound complexes with *Shewanella putrefaciens* CN32 (CN32). Plots A, C, and E represent the concentration of (A) dissolved, (C) sorbed, and (E) total Fe(II), respectively. Plots B, D, and F represent the fraction of (B) dissolved, (D) sorbed, and (F) total Fe(II) to the total Fe. Biotic control represents pure Fh incubated with CN32, and bacteria control represents the samples of only CN32. Symbols represent the average value of triplicate samples, and error bars represent the standard deviation. The model organic compounds include: benzoquinone (BQ), glucose (GL), glucosamine (GN), tyrosine (TN), alginate (AL) and amylose (AM).

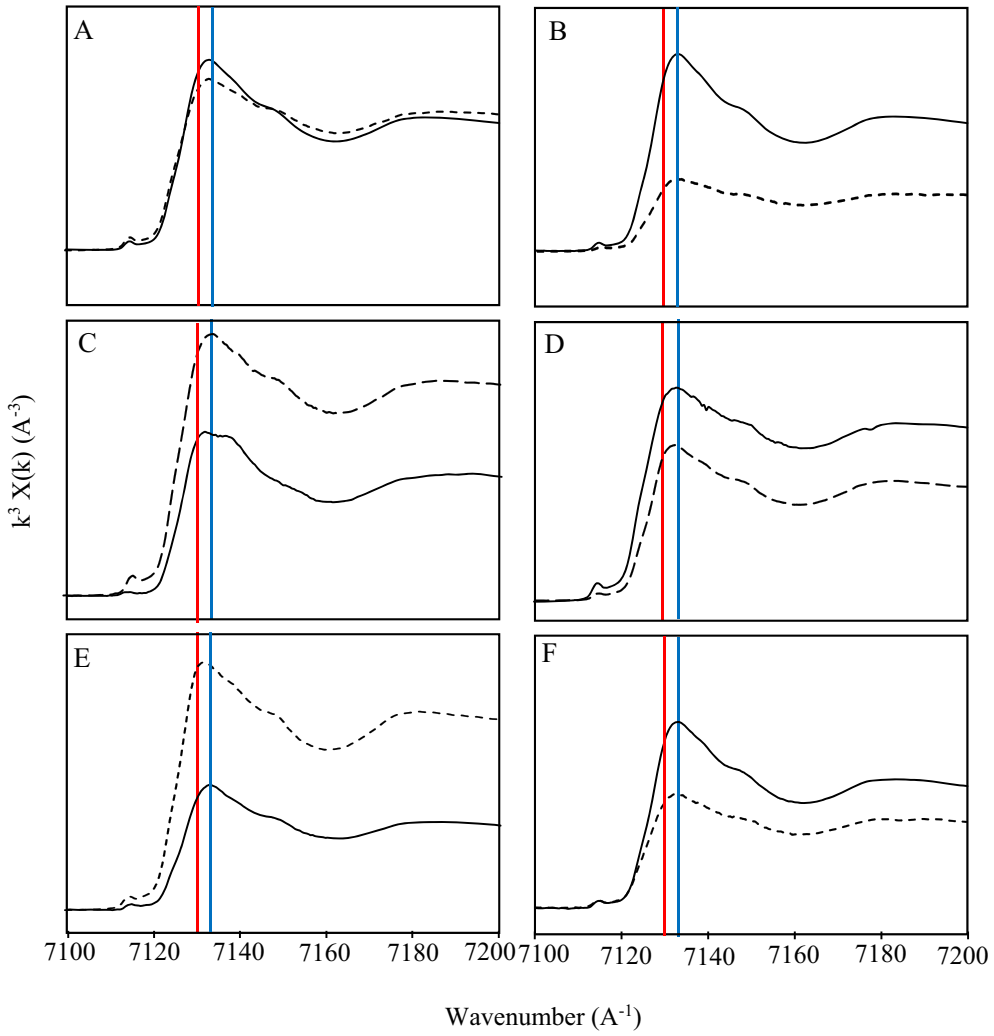

Fig. 2. X-ray absorption near edge structure (XANES) spectra of iron (Fe) in Fh-organic compound complexes before and after a 25-day anaerobic incubation. Solid and dashed lines represent samples of original Fh-organic compound complexes and those after anaerobic incubation, respectively. Blue and red vertical lines represent the white line positions for Fe(III) (7132 eV) and Fe(II) (7129 eV), respectively. The model organic compound complexes include: (A) Fh-BQ, (B) Fh-GL, (C) Fh-GN, (D) Fh-TN, (E) Fh-AL, and (F) Fh-AM. (For interpretation of the references to colour in this figure legend, the reader is referred to the web version of this article.)

3.4. Transformation of OC

During the anaerobic incubation, a minimal fraction of Fh-bound OC was oxidized to CO_2. On day 25, the concentration of CO_2 in the headspace of suspensions containing complexes was significantly higher than that in the biotic controls (*t-test*, $p < 0.05$), suggesting that oxidation of Fh-bound OC occurred (Fig. 5). The fraction of total C oxidized to CO_2 followed the order of Fh-GL (5.7%) > Fh-TN (4.3%) > Fh-GN (3.6%) > Fh-BQ (3.5%) > Fh-AM (3.3%) > Fh-AL (2.9%) (Fig. 5). Production of CH_4 was much lower, and there was no significant difference between the CH_4 concentration in the headspaces of suspensions with complexes and the biotic controls (*t-tests*, $p > 0.05$) (SI, Fig. S5). These results demonstrated that along with the release of Fh-bound OC into the solution phase, a portion of the Fh-bound OC and/or DOC was oxidized to CO_2. It is possible that the organic compounds were used as an electron donor for the reduction of Fe.

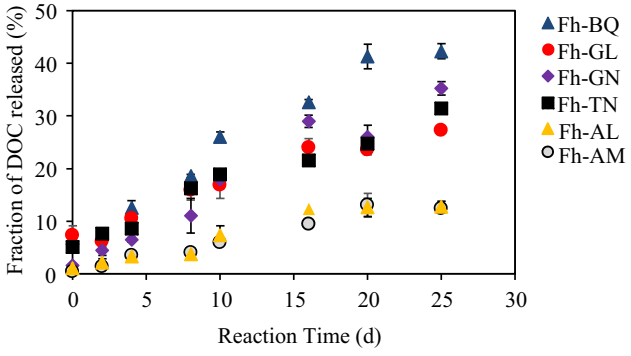

Fig. 3. Fraction of dissolved organic carbon (DOC) to total OC in the complexes during anaerobic incubation of Fh-model organic compound complexes with CN32. Symbols represent the average value obtained from triplicate experiments, and error bars represent the standard deviation. The DOC release from samples was calibrated based on the samples of biotic control.

4. Discussion

4.1. Impact of OC on Fe reduction

Organic carbon can regulate the reduction of Fe through multiple pathways: acting as an electron shuttle, affecting microbial activities, and associating with Fe oxides.

4.1.1. Electron shuttling process

Organic carbon has the potential to shuttle electrons between bacteria and minerals, i.e., microbially-reduced OC can abiotically donate

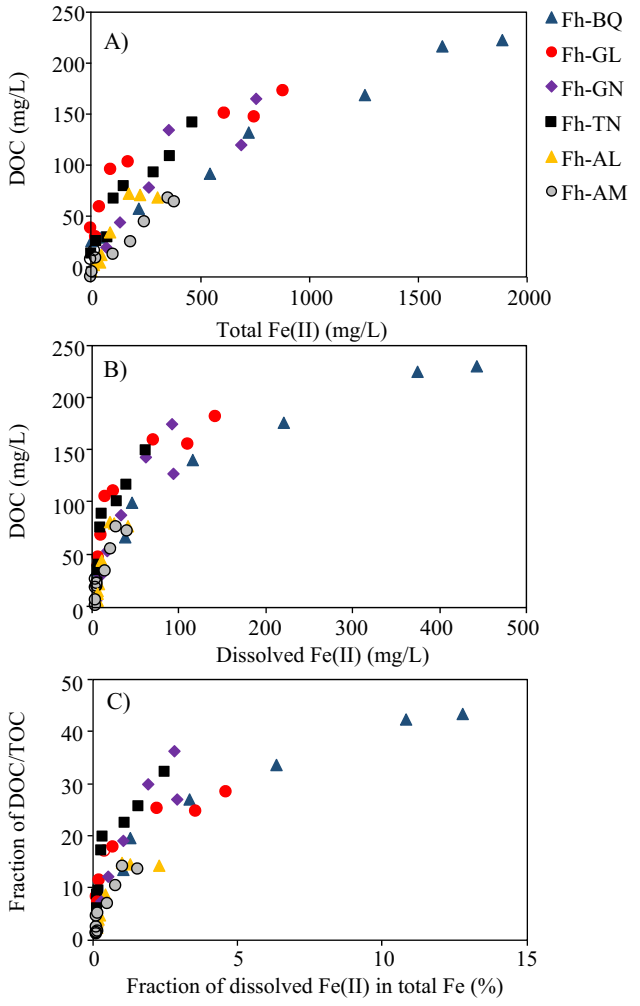

Fig. 4. Correlation between anaerobic iron reduction and carbon release. Plot A represents correlation between the amount of OC released and Fe reduction (total Fe(II)). Plot B represents the correlation between the amount of OC released and dissolved Fe(II). Plot C represents the correlation between the fraction of DOC/total organic carbon (TOC) in Fh-model organic compound co-precipitates and the fraction of dissolved Fe(II) to total Fe. The model organic compounds include: benzoquinone (BQ), glucose (GL), glucosamine (GN), tyrosine (TN), alginate (AL), and amylose (AM).

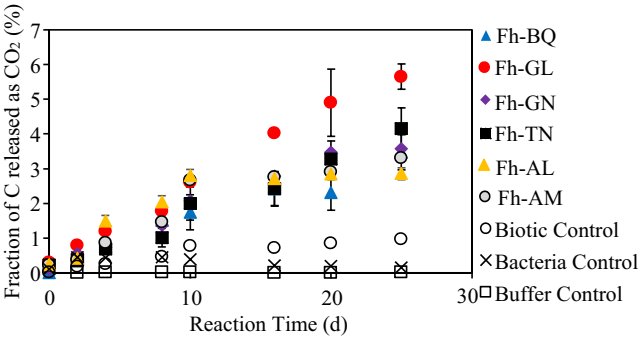

Fig. 5. Generation of CO_2, presented as the % of OC added in the complexes, for Fh-organic compound complexes anaerobically incubated with CN32. Symbols represent the mean of triplicate experiments, and error bars represent the standard deviation. The model organic compounds include: benzoquinone (BQ), glucose (GL), glucosamine (GN), tyrosine (TN), alginate (AL), and amylose (AM). The buffer control is a bacterium-, Fh-, and model compound-free sample containing only the buffer solution and is used here to determine the CO_2 background concentration resulting from sample preparation and buffer incubation.

electrons to Fe, reducing Fe(III) to Fe(II). We measured the EAC of BQ to be 0.313 mmol e^- equivalent $mol^{-1}C$, and EACs of other OC compounds were minimal with the next highest value of 0.05 mmol e^- equivalent $mol^{-1}C$ (SI, Fig. S6). Previous studies have assigned quinone moieties the most important component in natural OC for electron shuttling (Brose and James, 2010; Li et al., 2013). Using electron paramagnetic resonance (EPR) spectroscopy, Scott et al. (1998) demonstrated a significant correlation between the EAC of natural OC and quinone content. O'Loughlin (2008) have extensively analyzed the EAC of different quinone-containing compounds and have demonstrated strong positive correlations between the EAC and reduction potential of quinone moieties. Of the functional groups utilized in this study, our results indicated that only BQ, with a reduction potential of 0.28 V (Rau et al., 2002), can shuttle electrons between CN32 and Fh, providing direct evidence for the unique importance of quinone moieties in mediating the reduction of Fe minerals.

In addition, our comparison showed that the EAC of dissolved BQ was significantly higher than that for Fh-bound BQ (*t-test*, $p < 0.01$). EAC of Fh-bound BQ was only 46% of that for freely dissolved BQ (SI, Fig. S6, Table S4). Roden et al. (2010) measured the EAC of solid-phase organic matter, i.e., humic substances, and showed the EAC of solid-phase natural organic matter was approximately 10% of that for freely dissolved organic matter. The ratio we measured for Fh-bound BQ compared to freely dissolved BQ was similar. Binding between BQ and Fh, through van der Waals interactions and hydrogen bonding, can potentially decrease the EAC of BQ.

4.1.2. Impact of organic compounds on the microbial activity

Organic carbon can also affect bacterial activities. Most of the compounds tested can be used by CN32 as both carbon and energy sources. Based on the logistic model simulation, the lag phase was minimal, with λ smaller than 9 h. In the presence of LB only, the bacteria gradually grew to a stationary phase within 20 h, and started to decay after 48 h ($A = 8.84$, $\mu_m = 0.86$) (SI, Fig. S7, Table S5). With the addition of GL, the growth of CN32 was enhanced and did not demonstrate a decay phase within the first 98 h of incubation. Addition of GN and AM reduced the maximum specific growth rate. The addition of BQ, however, inhibited the growth of CN32 by decreasing the maximal population size. To further demonstrate this, CN32 cells grown in LB media were harvested and re-suspended in a buffer solution containing one model compound. The results (Fig. S7B) show that CN32 in GL and GN solutions continue to grow within the first 70 h, but gradually decay in BQ, TN, and AM solutions. CN32 in the presence of BQ demonstrated the most rapid decay in optical density, indicating that BQ likely inhibits the function of or is toxic to the cells. Roden and Zachara (1996) demonstrated that the rate of Fe reduction leveled off when the cells per surface area was above 10^9 cells m^{-2}. This indicates when the bacterial cell density is sufficiently high, electron shuttling processes dominated. These results are consistent with the highest reduction of Fe in the Fh-BQ samples in this study. When the bacterial cell density was low, the effects of organic compounds on microbial activity might regulate Fe reduction, together with other geochemical influences.

4.1.3. Associations between Fe oxides and organic compounds

In addition to the electron shuttling processes, associations between Fh and organic compounds can also affect Fe reduction. Ferrihydrite-GN demonstrated less Fe reduction compared to Fh-GL, possibly because of the presence of the amine group in GN and consequently stronger hydrogen bonding, which can be formed between Fe oxides and organic compounds. Ferrihydrite-TN had the lowest amount of Fe reduced among the complexes with low-molecular-weight compounds, which can be attributed to the presence of carboxylic groups and aromatic carbon interacting with Fe oxide through strong coordination complexation and aromatic ring-based interactions (Duckworth and Martin, 2001; Keiluweit et al., 2015; Strathmann and Myneni, 2004). When comparing GL and AM (with similar functional groups), a lower amount

of Fe was reduced in the presence of the higher molecular weight compound (AM), which might be resulted from stronger interactions between Fh and organic compounds due to their higher molecular weight. However, more Fe was reduced in Fh-AL than Fh-AM suspensions, although there are carboxylic groups in AL. This indicates the additional coordination complexation did not influence the reduction of Fe in Fh co-precipitated with high-molecular-weight organic compounds. The overall impact of associated organic compounds on Fe reduction is the combined result of Fe-organic compound interactions, effects on electron shuttling processes, and microbial activities. Reduction of Fe was highest for Fh-BQ, primarily contributed by the BQ-mediated electron shuttling; GL-impacted microbial activity potentially led to the second highest Fe reduction for Fh-GL; Fe reduction in Fh-AM was lowest among complexes, potentially because of relatively strong interactions between AM and Fh.

4.2. Release and transformation of organic compound

Strong correlations between Fe reduction and release of OC indicate that the release of OC is dominated by the reduction of Fe (Fig. 4, SI, Table S3), consistent with our recent work for natural soils and Fh co-precipitated with natural soil OC (Adhikari et al., 2016, 2017; Zhao et al., 2017). Adhikari et al. (2017) determined that the reduction of Fh and release of Fh co-precipitated OC were regulated by the C/Fe ratio of the complexes, with relatively higher C/Fe ratios facilitating Fe reduction and the reductive release of OC. In this study, such correlation between Fe reduction and OC release to the solution phase was demonstrated among model organic compounds with different functional groups and molecular weights. These findings cohesively demonstrate the importance of Fe reduction in the mobilization of OC under anaerobic conditions and its consequent degradation, assuming that dissolved OC has higher bioavailability and degradation potential compared to the sorbed compartments (Adhikari et al., 2019a).

In terms of relative release of OC measured as PRI, generally the high-molecular-weight organic compounds (AL, AM) had lower PRIs compared to low-molecular-weight compounds. However, GN and TN had relatively higher PRIs, although they had additional functional groups, such as carboxylic, amine, and aromatic domains, which potentially are able to bind with Fe oxide strongly. This indicates that other geochemical factors, for instance the conformation of complexes, in addition to the chemical bond between OC and Fe oxide minerals influenced the reductive release of OC. The PRI was lower for AL compared to AM, potentially due to the carboxylic groups in AL. The generation of CO_2 was also lower for high-molecular-weight compounds compared to other low-molecular-weight OC. Among the low-molecular-weight compounds, the generation of CO_2 was highest for GL and lowest for BQ, consistent with their impact on the bacteria growth. Generation of CO_2 by TN was higher than GN, although there were aromatic and carboxylic groups in TN. Similar to the trends for PRI, the oxidation of AL was lower than AM. In the previous studies for aerobic incubation, GL has been demonstrated as relatively unstable OC in the soil, with higher fraction of mineralization within short period (~70% within a week); mineralization of AM was shown also quick although slower than GL (Koegel-Knabner, 2002, 2017). There is relatively limited information about the fate of OC during anaerobic processes. Huang and Hall showed that anaerobic reduction of Fe can facilitate the mineralization of OC after 25-day incubation, with dominant contribution from mineralization of older C3 plant-derived C. The exact role of functional groups in generation of CO_2 from model organic compounds requires further investigation.

5. Conclusion

Differential impacts of various model organic compounds with different functional groups on the reduction of co-precipitated Fh were demonstrated in this study. The reduction of Fe followed the order of Fh-BQ > Fh-GL > Fh-GN > Fh-TN > Fh-AL > Fh-AM. BQ can shuttle electrons to facilitate the reduction of Fh, but can also potentially inhibit the activities of bacterial cells. Glucose and GN can be used as bacterial carbon and energy sources to promote microbial activities. The overall impacts of co-precipitated organic compounds on the reduction of Fh were derived from the combined influences of electron shuttling processes and microbial activities as well as Fe-organic compound associations. The reductive release of OC was closely correlated with the reduction of Fe. During the anaerobic incubation, a small fraction of the organic compounds were oxidized to CO_2, with CO_2 generation highest from Fh-GL complexes, consistent with glucose's role as both an energy and carbon source for bacteria. This study has shown dissimilar dynamics of Fe and OC in Fh- organic compounds complexes, depending on the organic functional groups. Such results are valuable for understanding the coupled biogeochemical cycles of Fe and soil OC. We provided evidence for the dissimilar fate of mineral-bound different groups of OC during anaerobic reactions.

Declarations of interest

None.

Acknowledgements

This research was financially supported by University of Nevada-Reno Startup fund, DOE grant DE-SC0014275 and USDA grant 2015-67018-23120.

Appendix A. Supplementary data

Supplementary data to this article can be found online at https://doi.org/10.1016/j.scitotenv.2019.02.441.

References

Adhikari, D., Yang, Y., 2015. Selective stabilization of aliphatic organic carbon by iron oxide. Sci. Rep. 5, 1–7. https://doi.org/10.1038/srep11214.
Adhikari, D., Poulson, S.R., Sumaila, S., Dynes, J.J., McBeth, J.M., Yang, Y., 2016. Asynchronous reductive release of iron and organic carbon from hematite-humic acid complexes. Chem. Geol. 430, 13–20. https://doi.org/10.1016/j.chemgeo.2016.03.013.
Adhikari, D., Zhao, Q., Das, K., Mejia, J., Huang, R., Wang, X., Poulson, S.R., Tang, Y., Roden, E.E., Yang, Y., 2017. Dynamics of ferrihydrite-bound organic carbon during microbial Fe reduction. Geochim. Cosmochim. Acta 212, 221–233. https://doi.org/10.1016/j.gca.2017.06.017.
Adhikari, D., Dunham-Cheatham, S.M., Wordofa, D.N., Verburg, P., Poulson, S.R., Yang, Y., 2019a. Aerobic respiration of mineral-bound organic carbon in a soil. Sci. Total Environ. 651, 1253–1260. https://doi.org/10.1016/j.scitotenv.2018.09.271.
Adhikari, D., Sowers, T., Stuckey, J.W., Wang, X.L., Sparks, D.L., Yang, Y., 2019b. Formation and redox reactivity of ferrihydrite-organic carbon-calcium co-precipitates. Geochim. Cosmochim. Acta 244, 86–98. https://doi.org/10.1016/j.gca.2018.09.026.
Bose, S., Hochella, M.F., Gorby, Y.A., Kennedy, D.W., McCready, D.E., Madden, A.S., Lower, B.H., 2009. Bioreduction of hematite nanoparticles by the dissimilatory iron reducing bacterium Shewanella oneidensis MR-1. Geochim. Cosmochim. Acta 73, 962–976.
Brose, D.A., James, B.R., 2010. Oxidation-reduction transformations of chromium in aerobic soils and the role of electron-shuttling quinones. Environ. Sci. Technol. 44, 9438–9444. https://doi.org/10.1021/es101859b.
Chacon, N., Silver, W.L., Dubinsky, E.A., Cusack, D.F., 2006. Iron reduction and soil phosphorus solubilization in humid tropical forests soils: the roles of labile carbon pools and an electron shuttle compound. Biogeochemistry 78, 67–84.
Chen, C., Thompson, A., 2018. Ferrous iron oxidation under varying pO2Levels: the effect of Fe(III)/Al(III) oxide minerals and organic matter. Environ. Sci. Technol. 52, 597–606. https://doi.org/10.1021/acs.est.7b05102.
Chorover, J., Amistadi, M.K., 2001. Reaction of forest floor organic matter at goethite, birnessite and smectite surfaces. Geochim. Cosmochim. Acta 65, 95–109. https://doi.org/10.1016/S0016-7037(00)00511-1.
Cornell, R.M., 1985. Effect of simple sugars on the alkaline trasformation of ferrihydrite into goethite and hematite. Clays & Clay Minerals 33 (3), 219–227.
Cornell R.M., Schwertmann U., 1996. The Iron Oxides: Structure, Properties, Reactions, Occurrences and Uses. Federal Republic of Germany.
Dippold, M., Biryukov, M., Kuzyakov, Y., 2014. Sorption affects amino acid pathways in soil: implications from position-specific labeling of alanine. Soil Biol. Biochem. 2014 (72), 180–192. https://doi.org/10.1016/j.soilbio.2014.01.015.
Duckworth, O.W., Martin, S.T., 2001. Surface complexation and dissolution of hematite by C1-C6dicarboxylic acids at pH = 5.0. Geochim. Cosmochim. Acta 65, 4289–4301. https://doi.org/10.1016/S0016-7037(01)00696-2.

Fredrickson, J.K., Zachara, J.M., Kennedy, D.W., Dong, H.L., Onstott, T.C., Hinman, N.W., Li, S.M., 1998. Biogenic iron mineralization accompanying the dissimilatory reduction of hydrous ferric oxide by a groundwater bacterium. Geochim. Cosmochim. Acta 62, 3239–3257.

Gál, A., Vyn, T.J., Michéli, E., Kladivko, E.J., McFee, W.W., 2007. Soil carbon and nitrogen accumulation with long-term no-till versus moldboard plowing overestimated with tilled-zone sampling depths. Soil Tillage Res. 96, 42–51. https://doi.org/10.1016/j.still.2007.02.007.

Ginn, B., Meile, C., Wilmoth, J., Tang, Y.Z., Thompson, A., 2017. Rapid iron reduction rates are stimulated by high-amplitude redox fluctuations in a tropical forest soil. Environmental Science & Technology 51 (6), 3250–3259.

Grybos, M., Davranche, M., Gruau, G., Petitjean, P., 2007. Is trace metal release in wetland soils controlled by organic matter mobility or Fe-oxyhydroxides reduction? J. Colloid Interface Sci. 314, 490–501. https://doi.org/10.1016/j.jcis.2007.04.062.

Hall, S.J., Silver, W.L., Timokhin, V.I., Hammel, K.E., 2016. Iron addition to soil specifically stabilized lignin. Soil Biol. Biochem. 98, 95–98.

Han, L., Sun, K., Jin, J., Xing, B., 2016. Some concepts of soil organic carbon characteristics and mineral interaction from a review of literature. Soil Biol. Biochem. 94, 107–121. https://doi.org/10.1016/j.soilbio.2015.11.023.

Huang, W.J., Hall, S.J., 2017. Elevated moisture stimulates carbon loss from mineral soils by releasing protected organic matter. Nat. Commun. 8, 1774.

Huang, X.L., Tang, H.Y., Kang, W.J., Yu, G.H., Ran, W., Hong, J.P., Shen, Q.R., 2018. Redox interface-associated organo-mineral interactions: a mechanism for C sequestration under a rice-wheat cropping system. Soil Biol. Biochem. 120, 12–23.

Jambor, J.L., Dutrizac, J.E., 1998. Occurrence and constitution of natural and synthetic ferrihydrite a widespread iron oxyhydroxide. Chem. Rev. 98, 2549–2585.

Kaiser, K., Guggenberger, G., 2000. The role of DOM sorption to mineral surfaces in the preservation of organic matter in soils. Org. Geochem. 31, 711–725. https://doi.org/10.1016/S0146-6380(00)00046-2.

Kappler, A., Benz, M., Schink, B., Brune, A., 2004. Electron shuttling via humic acids in microbial iron(III) reduction in a freshwater sediment. FEMS Microbiol. Ecol. 47, 85–92.

Keiluweit, M., Bougoure, J.J., Nico, P.S., Pett-Ridge, J., Weber, P.K., Kleber, M., 2015. Mineral protection of soil carbon counteracted by root exudates. Nat. Clim. Chang. 5, 588–595. https://doi.org/10.1038/nclimate2580.

Koegel-Knabner, Ingrid, 2017. The macromolecular organic composition of plant and microbial residues as inputs to soil organic matter: fourteen years on. Soil Biol. Biochem. 105, A3–A8.

Kogel-Knabner, I., 2002. The macromolecular organic composition of plant and microbial residues as inputs to soil organic matter. Soil Biol. Biochem. 34, 139–162.

Lalonde, K., Mucci, A., Ouellet, A., Gélinas, Y., 2012. Preservation of organic matter in sediments promoted by iron. Nature 483, 198–200. https://doi.org/10.1038/nature10855.

Li, X., Liu, L., Liu, T., Yuan, T., Zhang, W., Li, F., Zhou, S., Li, Y., 2013. Electron transfer capacity dependence of quinone-mediated Fe(III) reduction and current generation by Klebsiella pneumoniae L17. Chemosphere 92, 218–224. https://doi.org/10.1016/j.chemosphere.2013.01.098.

Liptzin, D., Silver, W.L., 2009. Effects of carbon additions on iron reduction and phosphorus availability in a humid tropical forest soil. Soil Biol. Biochem. 41, 1696–1702.

Lovley, D.R., Phillips, E.J., 1986. Organic matter mineralization with reduction of ferric iron in anaerobic sediments. Appl. Environ. Microbiol. 51 (4), 683–689.

Lovley, D.R., Coates, J.D., BluntHarris, E.L., Phillips, E.J.P., Woodward, J.C., 1996. Humic substances as electron acceptors for microbial respiration. Nature 382, 445–448.

Luan, F., Burgos, W.D., Xi, E.L., Zhou, Q., 2010. Bioreduction of nitrobenzene, natural organic matter, and hematite by Shewanella putrefaciens CN32. Environ. Sci. Technol. 44, 184–190. https://doi.org/10.1021/es901585z.

Meersmans, J., van Wesemael, B., De Ridder, F., Van Molle, M., 2009. Modelling the three-dimensional spatial distribution of soil organic carbon (SOC) at the regional scale (Flanders, Belgium). Geoderma 152, 43–52. https://doi.org/10.1016/j.geoderma.2009.05.015.

Meshulam-Simon, G., Behrens, S., Choo, A.D., Spormann, A.M., 2007. Hydrogen metabolism in Shewanella oneidensis MR-1. Appl. Environ. Microbiol. 73, 1153–1165. https://doi.org/10.1128/AEM.01588-06.

Najem, T., Langley, S., Fortin, D., 2016. A comparison of Fe(III) reduction rates between fresh and aged biogenic iron oxides (BIOS) by Shewanella putrefaciens CN32. Chem. Geol. 439, 1–12. https://doi.org/10.1016/j.chemgeo.2016.06.006.

Newville, M., 2001. IFEFFIT: interactive XAFS analysis and FEFF fitting. J. Synchrotron Rad. 8, 322–324.

O'Loughlin, E.J., 2008. Effects of electron transfer mediators on the bioreduction of lepidocrocite (γ-FeOOH) by Shewanella putrefaciens CN32. Environmental Science & Technology 42, 6876–6882. https://doi.org/10.1021/es800686d.

Pan, W., Kan, J., Inamdar, S., Chen, C., Sparks, D., 2016. Dissimilatory microbial iron reduction release DOC (dissolved organic carbon) from carbon-ferrihydrite association. Soil Biol. Biochem. 103, 232–240. https://doi.org/10.1016/j.soilbio.2016.08.026.

Philippe, A., Schaumann, G.E., 2014. Interactions of dissolved organic matter with natural and engineered inorganic colloids: a review. Environ. Sci. Technol. 48, 8946–8962. https://doi.org/10.1021/es502342r.

Porras, R.C., Hicks Pries, C.E., Torn, M.S., Nico, P.S., 2018. Synthetic iron (hydr)oxide-glucose associations in subsurface soil: effects on decomposability of mineral associated carbon. Sci. Total Environ. 613–614, 342–351. https://doi.org/10.1016/j.scitotenv.2017.08.290.

Rau, J., Knackmuss, H.J., Stolz, A., 2002. Effects of different quinoid redox mediators on the anaerobic reduction of azo dyes by bacteria. Environmental Science & Technology 36 (7), 1497–1504.

Roden, E.E., 2003. Fe(III) oxide reactivity toward biological versus chemical reduction. Environ. Sci. Technol. 37, 1319–1324. https://doi.org/10.1021/es026038o.

Roden, E.E., 2004. Analysis of long-term bacterial vs. chemical Fe(III) oxide reduction kinetics. Geochim. Cosmochim. Acta 68, 3205–3216. https://doi.org/10.1016/j.gca.2004.03.028.

Roden, E.E., Zachara, J.M., 1996. Microbial reduction of crystalline iron(III) oxides: influence of oxide surface area and potential for cell growth. Environ. Sci. Technol. 30, 1618–1628. https://doi.org/10.1021/es9506216.

Roden, E.E., Kappler, A., Bauer, I., Jiang, J., Paul, A., Stoesser, R., Konishi, H., Xu, H., 2010. Extracellular electron transfer through microbial reduction of solid-phase humic substances. Nat. Geosci. 3, 417–421. https://doi.org/10.1038/ngeo870.

Scott, D.T., McKnight, D.M., Blunt-Harris, E.L., Kolesar, S.E., Lovley, D.R., 1998. Quinone moieties act as electron acceptors in the reduction of humic substances by humics-reducing microorganisms. Environ. Sci. Technol. 32, 2984–2989.

Scurlock, J.M.O., Hall, D.O., 2008. The global carbon sink: a grassland perspective. Glob. Chang. Biol. 4, 229–233. https://doi.org/10.1046/j.1365-2486.1998.00151.x.

Stookey, L.L., 1970. Ferrozine-a new spectrophotometric reagent for iron. Anal. Chem. 42, 779–781. https://doi.org/10.1021/ac60289a016.

Strathmann, T.J., Myneni, S.C.B., 2004. Speciation of aqueous Ni(II)-carboxylate and Ni(II)-fulvic acid solutions: combined ATR-FTIR and XAFS analysis. Geochim. Cosmochim. Acta 68, 3441–3458. https://doi.org/10.1016/j.gca.2004.01.012.

Taran, O., 2017. Electron transfer between electrically conductive minerals and quinones. Frontiers in Chemistry 5, 1–13. https://doi.org/10.3389/fchem.2017.00049.

Wagai, R., Mayer, L.M., 2007. Sorptive stabilization of organic matter in soils by hydrous iron oxides. Geochim. Cosmochim. Acta 71, 25–35. https://doi.org/10.1016/j.gca.2006.08.047.

Webb, S.M., 2005. SIXpack: a graphical user interface for XAS analysis using IFEFFIT. Phys. Scripta T115, 1011–1014.

Xu, S., Adhikari, D., Huang, R., Zhang, H., Tang, Y., Roden, E., Yang, Y., 2016. Biochar-facilitated microbial reduction of hematite. Environ. Sci. Technol. 50, 2389–2395. https://doi.org/10.1021/acs.est.5b05517.

Zhao, Q., Poulson, S.R., Obrist, D., Sumaila, S., Dynes, J.J., McBeth, J.M., Yang, Y., 2016. Iron-bound organic carbon in forest soils: quantification and characterization. Biogeosciences 13, 4777–4788.

Zhao, Q., Adhikari, D., Huang, R., Patel, A., Wang, X., Tang, Y., Obrist, D., Roden, E.E., Yang, Y., 2017. Coupled dynamics of iron and iron-bound organic carbon in forest soils during anaerobic reduction. Chem. Geol. 464, 118–126. https://doi.org/10.1016/j.chemgeo.2016.12.014.